

UC Santa Barbara

UC Santa Barbara Previously Published Works

Title

Effects of Surfactants and Polyelectrolytes on the Interaction between a Negatively Charged Surface and a Hydrophobic Polymer Surface

Permalink

<https://escholarship.org/uc/item/0rn550qp>

Journal

Langmuir, 31(29)

ISSN

0743-7463

Authors

Rapp, Michael V
Donaldson, Stephen H
Gebbie, Matthew A
[et al.](#)

Publication Date

2015-07-28

DOI

10.1021/acs.langmuir.5b01781

Peer reviewed

Effects of Surfactants and Polyelectrolytes on the Interaction between a Negatively Charged Surface and a Hydrophobic Polymer Surface

Michael V. Rapp,[†] Stephen H. Donaldson, Jr.,[†] Matthew A. Gebbie,[‡] Yonas Gizaw,[§] Peter Koenig,^{||} Yuri Roiter,[§] and Jacob N. Israelachvili^{*,†,‡}

[†]Department of Chemical Engineering, University of California, Santa Barbara, California 93106-5080, United States

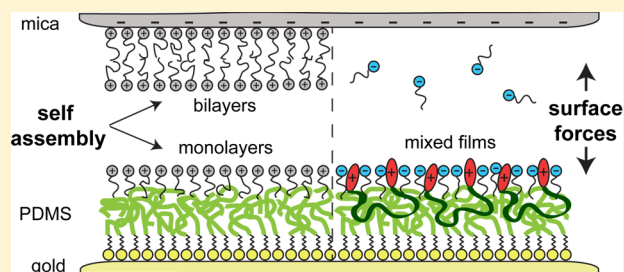
[‡]Materials Department, University of California, Santa Barbara, California 93106-5050, United States

[§]Winton Hill Business Center, The Procter & Gamble Company, 6210 Center Hill Avenue, Cincinnati, Ohio 45224, United States

^{||}Modeling and Simulation/Computational Chemistry, The Procter & Gamble Company, 8611 Beckett Road, West Chester, Ohio 45069, United States

Supporting Information

ABSTRACT: We have measured and characterized how three classes of surface-active molecules self-assemble at, and modulate the interfacial forces between, a negatively charged mica surface and a hydrophobic end-grafted polydimethylsiloxane (PDMS) polymer surface in solution. We provide a broad overview of how chemical and structural properties of surfactant molecules result in different self-assembled structures at polymer and mineral surfaces, by studying three characteristic surfactants: (1) an anionic aliphatic surfactant, sodium dodecyl sulfate (SDS), (2) a cationic aliphatic surfactant, myristyltrimethylammonium bromide (MTAB), and (3) a silicone polyelectrolyte with a long-chain PDMS midblock and multiple cationic end groups. Through surface forces apparatus measurements, we show that the separate addition of three surfactants can result in interaction energies ranging from fully attractive to fully repulsive. Specifically, SDS adsorbs at the PDMS surface as a monolayer and modifies the monotonic electrostatic repulsion to a mica surface. MTAB adsorbs at both the PDMS (as a monolayer) and the mica surface (as a monolayer or bilayer), resulting in concentration-dependent interactions, including a long-range electrostatic repulsion, a short-range steric hydration repulsion, and a short-range hydrophobic attraction. The cationic polyelectrolyte adsorbs as a monolayer on the PDMS and causes a long-range electrostatic attraction to mica, which can be modulated to a monotonic repulsion upon further addition of SDS. Therefore, through judicious selection of surfactants, we show how to modify the magnitude and sign of the interaction energy at different separation distances between hydrophobic and hydrophilic surfaces, which govern the static and kinetic stability of colloidal dispersions. Additionally, we demonstrate how the charge density of silicone polyelectrolytes modifies both their self-assembly at polymer interfaces and the robust adhesion of thin PDMS films to target surfaces.



1. INTRODUCTION

Surfactant adsorption is the most prevalent method to control the aqueous interfacial energy of both mineral and soft polymer surfaces.¹ Amphiphilic ionic surfactants have the versatility to adsorb and self-assemble at either a charged surface through electrostatic interactions with their polar headgroups, or at a hydrophobic surface through interactions with their nonpolar tails. In industrial separation and recovery processes—such as froth flotation, flocculation, and hydraulic fracturing—surfactants are vital additives that regulate the wettability and friction at mineral–water interfaces. In addition to their abundant use as grease-cleaning detergents, surfactants stabilize hydrophobic oil droplets in emulsions and cosmetics.^{2–5} Frequently, consumer products and industrial separation techniques employ a mixture of surfactants, polymers, and polyelectrolytes in synergy to achieve a desired behavior of an end product.^{3–13}

A tremendous variety of useful surfactants exist. The properties of specific classes of surfactants, and the resultant engineering functions of these surfactants, depend on differences in the surfactant structure (lipid, gemini, or bolaform surfactants), the size and number of the nonpolar tails (ranging from short aliphatic chains to long polymer chains), or the headgroup charge (anionic, cationic, nonionic, zwitterionic, polymeric, or polyelectrolyte surfactants).¹⁴ At a surface, surfactants self-assemble into different interfacial structures—such as monolayers, bilayers, hemicylinders, or hemimicelles—based on the innate chemical and physical characteristics of both the surfactant and the surface, as well as the solution

Received: May 14, 2015

Revised: July 1, 2015

Published: July 2, 2015

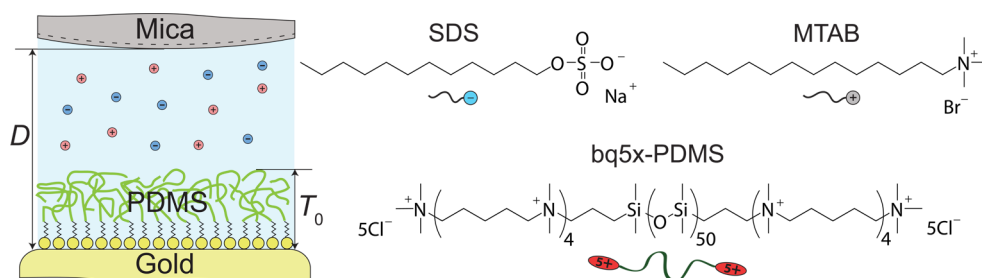


Figure 1. Schematic of the experimental setup in the SFA and the surfactant molecules used in this study. In an aqueous solution, a mica surface approaches and separates normal to a covalently grafted PDMS surface on gold. In separate experiments, these surfaces are subsequently modified by the addition of anionic SDS surfactants, cationic MTAB surfactants, or cationic bq5x-PDMS polyelectrolytes.

concentration.^{15–21} Correspondingly, the self-assembled structures modulate the interaction forces between surfaces in solution, controlling the stabilization, flocculation, viscosity, lubrication, or adhesion of colloidal suspensions and macroscopic surfaces.

In a previous study using the surface forces apparatus (SFA), we demonstrated that a long-chain polydimethylsiloxane (PDMS) bolaform surfactant (bq-PDMS) adsorbs onto grafted-PDMS polymer brush surfaces and forms dynamically fluctuating nanostructures that protrude tens of nanometers into solution.²² These soft nanostructures behave analogously to surface-tethered polymers exposed to bulk solution and give rise to rate-dependent attractive and adhesive forces on the approach and separation of another surface. These nanostructures represent a unique subset of self-assembled films that presumably exist for only certain surfactant–surface combinations; small changes to the surfactant length or charge are expected to result in different self-assembly and force profiles at polymer surfaces.

In this study, we extend our previous work to explore how three classes of surfactants self-assemble at, and modulate the surface forces between, a negatively charged mineral surface (mica) and a hydrophobic polymer surface (PDMS) in aqueous solution (Figure 1). The three surfactants used in this study were selected for their wide range of chemical and structural properties: (1) sodium dodecyl sulfate (SDS), a characteristic anionic aliphatic surfactant, (2) myristyltrimethylammonium bromide (MTAB), a characteristic cationic aliphatic surfactant, and (3) bq5x-PDMS, a polyelectrolyte similar in structure to the previously studied bq-PDMS, but with a 5-fold increase in the end group charge density. Measurements were performed in single-component surfactant solutions, as well as a binary mixture of SDS and bq5x-PDMS. Overall, the resulting self-assembled structures and measured forces between these interfaces provide a broad overview of surfactant behavior at polymer and mineral surfaces. This comprehensive understanding of surfactant–polymer–surface interactions establishes design parameters for functionalized interfaces in consumer products and industrial applications.

2. EXPERIMENTAL SECTION

Surface forces measurements were performed with the SFA 2000, manufactured by SurForce LLC., Santa Barbara, California. The full details of the SFA technique may be found elsewhere.²³ Briefly, the interaction force (F) between two crossed-cylinder surfaces (radius, $R \sim 2$ cm) is measured as a function of the separation distance (D) between two surfaces. The two surfaces used in this study are (1) a freshly cleaved, back-silvered mica surface, and (2) a molecularly-smooth gold surface that has been covalently grafted with a hydrophobic PDMS brush film. The absolute separation distance

between the surfaces is measured with multiple beam interferometry between the reflecting gold and silver layer on mica.

At the start of an experiment, a pristine mica and gold surface (without a grafted film) were installed in the SFA and brought into molecular contact in dry N_2 ; this separation distance was assigned $D = 0$. The pristine gold surface was then replaced in the SFA with a gold surface that had been grafted with a PDMS film, and the chamber of the SFA was filled with degassed aqueous solution (typically 1 or 5 mM NaCl). The presence of interfacial nanobubbles was never observed at the PDMS surface. The system was allowed to equilibrate until thermal and mechanical drift in the SFA were negligible, and force measurements were performed by the normal approach and separation of the mica and PDMS surfaces at a rate of ~ 2 nm/s. The interaction forces between the surfaces at all distances were calculated from the deflection of a double-cantilevered spring that held one of the two surfaces. For comparison between differing experiments, all forces in this study were normalized by the radius (F/R), and when appropriate, the measured interaction force was converted into an interaction energy using the Derjaguin approximation ($W = F/2\pi R$) or an adhesion energy using the Johnson–Kendall–Roberts theory ($W_{ad} = F_{ad}/1.5\pi R$).²⁴ All force measurements in this study were reproduced over multiple experiments, and represent the quasi-equilibrium interaction forces between the surfaces.

PDMS films were prepared as previously described.²⁵ Briefly, molecularly smooth gold surfaces were prepared via a mica templating technique.^{26,27} An amine-functionalized self-assembled monolayer (SAM) was adsorbed onto the gold surface through immersion in a 1 mM solution of 11-amino-1-undecanethiol hydrochloride (Sigma-Aldrich) in ethanol for 2 h. The SAM surfaces were rinsed in ethanol, dried in N_2 , and then submerged in neat monoglycidyl ether-terminated polydimethylsiloxane (Sigma-Aldrich, MW = 5000 g/mol) at 130 °C for 1 h. In this step, the PDMS polymers were covalently grafted to the SAM layer through a click reaction between the PDMS epoxide ring and the SAM terminal amine. At 130 °C, some fraction of the SAM film may have desorbed from the gold surface; however, the PDMS length and grafting density were large enough to ensure uniformly dense brush films that were free from holes. The click reaction may also be performed at lower temperatures with longer reaction times.²⁸ Following the reaction, unbound PDMS was removed from the gold surface through a cycle of rinsing and sonicating in toluene. Slight variations in the PDMS grafting density between sample preparations resulted in a total SAM + PDMS film thickness (T_0) that varied from ~ 6 to 10 nm between separate experiments; while the thickness of the film varied slightly among separate surfaces, the thickness of a film on a single surface was uniform.

Sodium dodecyl sulfate (SDS) and myristyltrimethylammonium bromide (MTAB) were purchased from Sigma-Aldrich. In experiments with SDS or MTAB, force measurements were first performed between the PDMS and mica surface at a specific contact point in a surfactant-free solution, to ascertain a baseline film thickness and interaction in aqueous solution. The aqueous reservoir between the two surfaces was then exchanged with a particular solution of SDS or MTAB, the system was allowed to equilibrate for ~ 1 h, and force runs

were performed between the surfaces at the same contact position as in the surfactant-free measurements.

Bq5x-PDMS (MW = 4842 g/mol) was provided by the Procter & Gamble Company (Cincinnati, Ohio). Bq5x-PDMS was dispersed in aqueous solution (1 NaCl, pH ~ 9) at a concentration of $\sim 6 \times 10^{-5}$ moles bq5x-PDMS/L; at this concentration, bq5x-PDMS formed aggregates of ~ 400 nm in diameter, as measured by dynamic light scattering (DLS). In the SFA experiments presented in this study, bq5x-PDMS was adsorbed onto only the PDMS surface. First, freshly prepared PDMS surfaces on gold were immersed in a small vial (~ 2 mL) of the bq5x-PDMS solution for 1.5 h. A solvent exchange procedure was then performed to deplete any nonadsorbed bq5x-PDMS aggregates from the reservoir, without ever exposing the PDMS surface to air and perturbing the adsorbed state of the bq5x-PDMS film. After the adsorption step, the entire small vial was (1) submerged within a larger vial (30 mL) of 1 mM NaCl, (2) gently mixed for 1 min, and (3) removed from the larger vial with a 15 \times diluted reservoir surrounding the PDMS surface. This solvent exchange procedure was repeated 7 times for each surface. The PDMS surface was then transferred under solution into the SFA for force measurements.

3. RESULTS AND ANALYSIS

3.1. Anionic Surfactant Monolayers. The headgroups of anionic surfactants, such as SDS, are repelled from the negatively charged mica surface, so little to no adsorption occurs on mica regardless of the bulk surfactant concentration. On a PDMS surface, the hydrophobic chains of SDS adsorb into the hydrophobic polymer layer of the PDMS thin film, resulting in a negatively charged SDS surface. Generally, hydrophobic surfaces display a negative surface charge at basic pH in aqueous solution,^{29,30} and their interactions are repulsive with a likewise negatively charged mica surface. As shown in Figure 2, the addition of SDS above the critical micelle concentration ($CMC_{SDS} = 8.2$ mM) modifies the magnitude, decay length, and plane of origin of the repulsion between mica and PDMS thin films. Without SDS (blue points), the interaction is mainly an electrostatic double-layer repulsion,

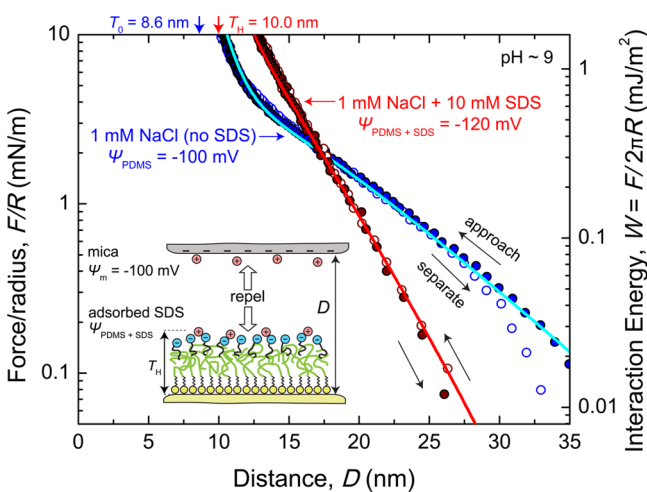


Figure 2. Interaction forces between a PDMS surface and a mica surface in a solution of SDS. SFA measurements were performed in a 1 mM NaCl solution at pH = 9, both before (blue data points) and after (red data points) 10 mM SDS was injected into the gap solution between the surfaces. Closed and open circles represent data measured on the approach and separation of the two surfaces, respectively. The corresponding solid curves passing through the data represent the fits with eq 1 using the surface potentials shown in the figure. Arrows at the top of the figure indicate the “hardwall” film thicknesses measured at maximum compression (T_H).

with a steric-hydration component at small separations. As described in our previous work, these forces can be modeled as a combination of van der Waals, asymmetric electrostatic double-layer, and steric-hydration using the model shown in eq 1.²⁵

$$W(D) = -\frac{1}{12\pi} \left(\frac{A_{mPg}}{D^2} + \frac{A_{mwP}}{(D - T_H)^2} \right) + \varepsilon \varepsilon_0 \kappa \left[\frac{2\psi_m \psi_p e^{-\kappa(D-T_H)} - (\psi_m^2 + \psi_p^2) e^{-2\kappa(D-T_H)}}{1 - e^{-2\kappa(D-T_H)}} \right] - 2\gamma_i \cdot Hy \cdot e^{-(D-T_H)/D_H} \quad (1)$$

For consistency, the equations presented herein are reported as the interaction energy, W , as a function of separation distance, D . T_H is the measured film thickness under maximum compression, i.e., the “hardwall” thickness. The first term in eq 1 is the van der Waals term; the Hamaker constants, A , were calculated according to Lifshitz theory¹⁴ as previously described for mica (m) and gold (g) interacting across PDMS (P), $A_{mPg} = 3.4 \times 10^{-20}$ J, and mica and PDMS interacting across water (w), $A_{mwP} = 7.1 \times 10^{-21}$ J. The second term is the electrostatic term for asymmetric double-layers interacting at constant potential^{31,32} with surface potentials ψ_m and ψ_p for the mica and PDMS surfaces, respectively. The Debye length κ^{-1} was calculated from eq 2

$$\kappa^{-1} = (\varepsilon_0 \varepsilon k T / 2N_A [\text{NaCl}] e^2)^{1/2} \quad (2)$$

where ε is the dielectric constant of water, ε_0 is the vacuum permittivity, N_A is Avogadro’s number, e is the fundamental charge, k is Boltzmann’s constant, and T is the absolute temperature. The third term in eq 1 is the steric-hydration term. As described in our previous work, the Hydra parameter Hy is used to quantify the relative hydrophilicity ($Hy < 0$) or hydrophobicity ($Hy > 0$) of interfaces.^{25,28} The Hydra parameter Hy is a measure of the excess hydrophobic or hydrophilic area at an interface: $Hy \equiv 1 - a_0/a$, where a is the hydrophobic area and a_0 is the hydrophilic area, with $Hy = 1$ corresponding to no additional hydrophobic or hydrophilic force, and $Hy < 0$ corresponding to a hydrophilic interaction.^{28,33} D_H is the decay length of the hydrophobic/hydrophilic interaction (generally D_H is between 0.3 and 2 nm depending on the system). In this case, $Hy < 0$ models the observed repulsive steric-hydration force, with a hydration decay length of $D_H \sim 1$ nm and a hydrocarbon–water interfacial tension of $\gamma_i = 50$ mJ/m².

In the absence of SDS, the interaction between mica and PDMS is described with a Hydra parameter of $Hy = -0.2 \pm 0.06$, a PDMS surface potential of $\psi_p = -100 \pm 20$ mV, and a mica surface potential of $\psi_m = -100 \pm 10$ mV, with a fitted screening length of $\kappa_{fit}^{-1} = 7.0 \pm 0.5$ nm (theoretical $\kappa^{-1} = 9.6$ nm). Increasing the NaCl concentration from 1 to 10 mM does not significantly alter ψ_m , however ψ_p decreases to -40 ± 10 mV at 10 mM NaCl.²⁵ The addition of 10 mM SDS modifies the PDMS surface potential and the electrostatic decay length (red points, Figure 2), to $\psi_p = -120 \pm 20$ mV and $\kappa^{-1} = 3.1$ nm (with $Hy = -0.24 \pm 0.1$). Thus, SDS adsorption preserves a high surface potential at the PDMS interface even in solutions of increased ionic strength. The self-assembly of SDS also shifts the hardwall distance from $T_H = 8.6$ nm in the absence of SDS, to $T_H = 10$ nm in the presence of SDS. The difference of 1.4

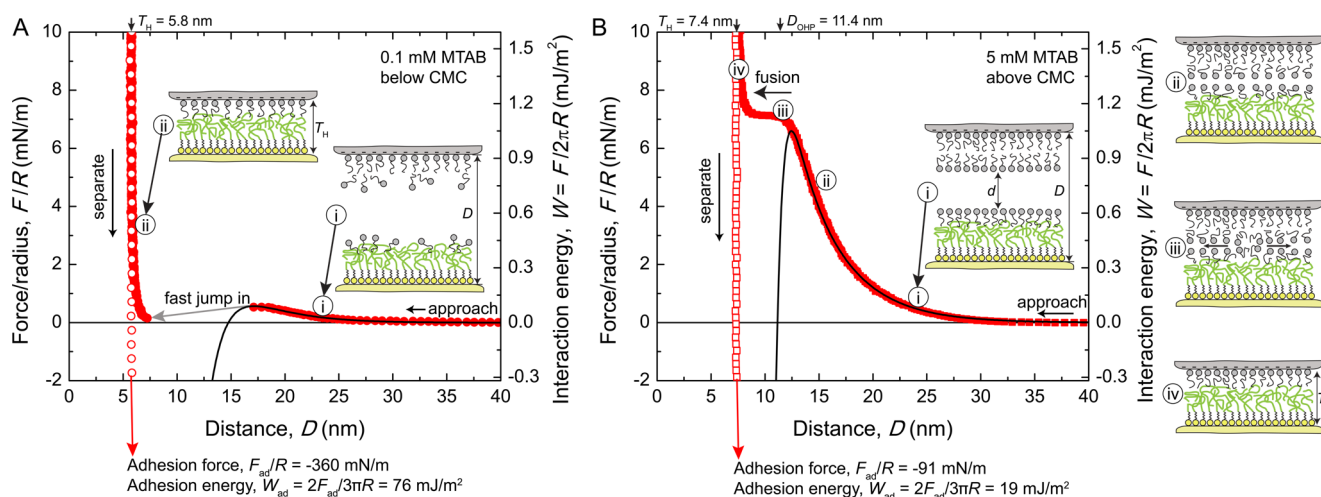


Figure 3. Interaction forces between a PDMS surface and a mica surface in a solution of cationic MTAB surfactants. The MTAB adsorbs to both the mica and PDMS surfaces. (A) 0.1 mM MTAB ($C < \text{CMC}_{\text{MTAB}}$). The interactions and mechanisms are shown in schematic drawings (i) and (ii) and described in detail in the text. (B) 5 mM MTAB ($C > \text{CMC}_{\text{MTAB}}$). The structural transformations of the adsorbed layers are shown in schematic drawings (i), (ii), (iii), and (iv) and described in detail in the text. In A and B, the solid black curves passing through the data represent the fits with eqs 3 and 5, respectively.

nm is the approximate length of a SDS molecule; however, from the force measurements, we are unable to determine if this shift out in the hardwall is due to a SDS monolayer that lies on top of the PDMS film, or due to a partially interdigitated SDS monolayer that swells the PDMS film. The overall analysis indicates that the addition of SDS results in SDS adsorption—either monolayer or interdigitated monolayer—to the PDMS film, primarily inducing a modification to the electrostatic double-layer force between the mica and PDMS surface.

3.2. Cationic Surfactant Monolayers and Bilayers.

Cationic surfactants modify both the mica and the PDMS surface. The cationic headgroups of the surfactants adsorb to the negatively charged mica surface, resulting in a monolayer or an incomplete bilayer on the mica at $C < \text{CMC}$, and a complete fluid bilayer at $C \gtrsim \text{CMC}$ ($\text{CMC}_{\text{MTAB}} = 3.7 \text{ mM}$).^{1,15,34} On the PDMS surface, the hydrophobic surfactant tails adsorb, either into or onto, the hydrophobic PDMS chains, with a dilute monolayer forming at $C < \text{CMC}$ and a dense monolayer at $C \gtrsim \text{CMC}$.^{1,17,19} Accordingly, the forces between a PDMS surface and a mica surface modified by adsorbed layers of cationic surfactant are dependent on the solution concentration of the cationic surfactant, as shown in Figure 3.

When $C < \text{CMC}$ (Figure 3A), a long-range repulsion is measured during approach of the surfaces, followed by an instability jump-in to contact. The surfaces adhere strongly, with an adhesion energy of $W_{\text{ad}} = 76 \text{ mJ/m}^2$ measured upon separation. The repulsion on approach can be described by the electrostatic double-layer interaction. There are two potential explanations for the attractive (adhesion) force, which is much stronger than the van der Waals force: hydrophobic interactions between the adsorbed monolayer on the mica and the PDMS film,³⁵ and/or a subtle charge regulation mechanism in which surfactants exchange during approach and result in an attractive electrostatic force.^{36,37} The adhesion, however, appears to be primarily due to a hydrophobic interaction, as the strong measured adhesion energy of $W_{\text{ad}} = 76 \text{ mJ/m}^2$ is close to the theoretical adhesion energy between two hydrophobic surfaces, $W_0 = 2\gamma_i = 80\text{--}100 \text{ mJ/m}^2$.¹⁴ Without further evidence of the charge regulation mechanism, the attractive force is quantita-

tively described by the recently proposed Hydra model for hydrophobic interactions.^{25,28}

The theoretical model (black line, Figure 3A) includes contributions from van der Waals, electrostatics, and hydrophobic interactions, as described by eq 3.

$$W_{\text{tot}}(D) = -\frac{1}{12\pi} \left(\frac{A_{\text{mPg}}}{D^2} + \frac{A_{\text{swP}}}{(D - T_H)^2} \right) + \frac{\kappa Z}{2\pi} e^{-\kappa D} - 2\gamma_i \cdot \text{Hy} \cdot e^{-(D - T_H)/D_H} \quad (3)$$

The double-layer interaction is treated as a constant potential interaction with symmetric potentials. The Hamaker constant for mica-bound surfactant and PDMS interacting across water, $A_{\text{swP}} = 4.4 \times 10^{-21} \text{ J}$, was calculated as previously described.¹⁴ The Debye length κ^{-1} was calculated from eq 2, and the interaction constant Z is calculated from eq 4

$$Z = 64\pi\epsilon_0\epsilon(kT/e)^2 \tan h^2(z\psi_0/4kT) \quad (4)$$

where ψ_0 is the symmetric surface potential, $z = 1$ is the ion valency, and all other variables are given above. $T_H = 5.7 \text{ nm}$ is the hardwall thickness. The salt concentration is 5.1 mM (5 mM NaCl plus 0.1 mM MTAB), giving a theoretical Debye length of $\kappa^{-1} = 4.3 \text{ nm}$. The long-range repulsion can be fitted by using the theoretical Debye length and adjusting ψ_0 to find $\psi_0 = 78 \text{ mV}$. Fitting the short-range attraction to the jump-in distance and adhesion shows that $D_H = 1.5 \text{ nm}$ and $\text{Hy} = 0.8$. Because $\text{Hy} = 1$ corresponds to two fully hydrophobic surfaces (maximum hydrophobic attraction), the measured value of $\text{Hy} = 0.8$ indicates that there could be some degree of overturned surfactants on the cationic monolayer or trapped surfactants upon adhesion.

For surfactant concentrations above the CMC, a fluid MTAB bilayer adsorbs on the mica and a densely packed MTAB monolayer adsorbs into the PDMS layer. The interaction forces now resemble the interactions measured between two fusing lipid bilayers,^{33,38,39} as shown in Figure 3B. The adsorbed layers first approach each other and interact through a long-range electrostatic interaction (Figure 3B(i)). As the approach continues and additional force is applied, the layers experience

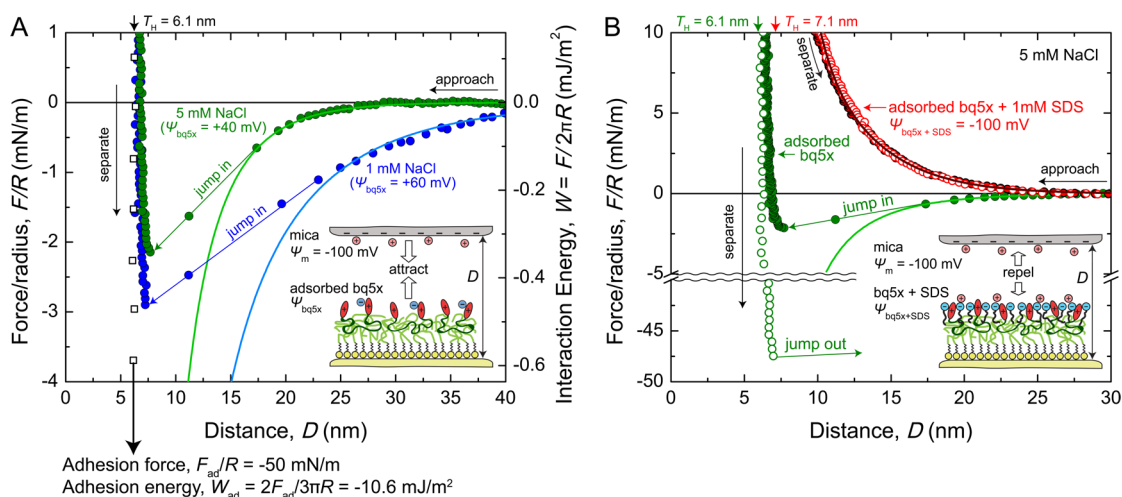


Figure 4. (A) Interaction forces between a PDMS surface preadsorbed with cationic bq5x-PDMS surfactant and a mica surface. SFA measurements were performed in 1 mM (closed blue circles) and 5 mM (closed green circles) NaCl solutions. As the surfaces approach, an electric double-layer attraction is measured until the gradient of the interaction becomes larger than the SFA spring constant, and the surfaces jump into adhesive contact (indicated with arrows). Strong adhesion is measured between the surfaces as they are separated (open black squares). (B) Addition of 1 mM SDS (red data points) reverses the charge at the bq5x-PDMS interface, and a monotonic repulsion is measured. The green data points (5 mM NaCl, no SDS) are repeated from A for comparison. Closed and open circles represent data measured on the approach and separation of the two surfaces, respectively. In both A and B, the corresponding solid curves passing through the data represent the fits with eq 7 using the surface potentials shown in the figure.

an additional repulsion due to steric-hydration forces, resulting in large normal stresses on the layers, which begin to squeeze and spread (Figure 3B(ii)). This spreading exposes the hydrophobic interior, eventually leading to an instability where the hydrophobic attraction overwhelms the strong steric and electrostatic repulsions, causing the outer surfactant layers to be pushed out (Figure 3B(iii)). This squeeze-out event leads to adhesive contact between the hydrophobic inner layers (monolayer of MTAB in contact with PDMS) (Figure 3B(iv)).

The fusion process was modeled previously for surfactant bilayers, and a similar analysis is applied here, as the physics appear to be nearly identical.^{33,40} The model is similar to eq 3 above, with extra terms for the bilayer stretching energy and steric-hydration repulsion. As shown in eq 5, the total interaction energy $W(d)$ for bilayer fusion is quantitatively described as a sum of bilayer stretching, hydrophobic interactions, electrostatic interactions, and steric hydration repulsion. Note that the theoretical model $W(d)$ is calculated as a function of the bilayer–bilayer distance, d , while the forces are plotted as a function of the mica–gold separation distance, D . The constant thickness of the PDMS and inner monolayer on mica, $T_H = 6$ nm, must be added to the variable thickness of the two outer layers that stress during the experiment, $T(d) = a(d)/v_0$, where v_0 was found from $a_0 l_0$ ($l_0 = 2$ nm is the surfactant chain length), such that $D = d + T_H + 2T(d)$. The calculated $W(d)$ is plotted vs D to compare with the measurements. In this case, the Hydra parameter is a function of distance as the surfactant layers are stressed: $Hy(d) \equiv 1 - a_0/a(d)$, where $a_0 = 45 \text{ \AA}^2$ is the equilibrium surfactant headgroup area and $a(d)$ is the stressed headgroup area, calculated as shown in eq 6. The hydrophobic force acts at the plane just beneath the surfactant headgroups, so the plane of origin for the hydrophobic force is shifted in by a total of 2δ , where $\delta = 0.2$ nm is the approximate thickness of the headgroup. As the layers are stressed, $a(d)$ increases from a_0 and the hydrophobic interaction becomes dominant at small separations.

$$W(d) = \left(2\gamma_i \frac{a_0^2}{a(d)^2} - 2\gamma_i \right) - 2\gamma_i Hy(d) \cdot e^{-(d+2\delta)/D_H} + \frac{C_{ES}}{a(d)} e^{-\kappa d} + \frac{C_{SHR}}{a(d)} e^{-d/D_{SHR}} \quad (5)$$

$$a(d) = a_0 (1 - e^{-(d+2\delta)/D_H})^{-1/2} \quad (6)$$

The electrostatics are determined in the limit of large d , such that $C_{ES}/a_0 = \kappa Z/2\pi$, allowing for calculation of the surface potential ψ_0 as shown in eq 4. The steric hydration pre-exponential term, C_{SHR} , and steric-hydration decay length, D_{SHR} , are fitted in the steep repulsion regime. Here, the total salt concentration is 5 mM MTAB (no background electrolyte), so $\kappa^{-1} = 4.3$ nm, and the fitted $C_{ES} = 1 \times 10^{-21}$ J, corresponding to $\psi_0 = 110$ mV. The remaining parameters are $D_H = 1$ nm, $\gamma_i = 50 \text{ mJ/m}^2$, $C_{SHR} = 3.1 \times 10^{-20}$ J with $D_{SHR} = 1$ nm.

As shown, the model captures the long-range forces, the short-range forces, and the force magnitude of the breakthrough event (instability). The predicted adhesion energy is $\sim 42 \text{ mJ/m}^2$, much larger than the measured adhesion of 19 mJ/m^2 . This discrepancy occurs because there is a surfactant reservoir in solution, thus surfactants can reassemble in the contact region during the separation, decreasing the interfacial energy γ_i of the hydrophobic interface. Nonetheless, the model is robust and captures most of the quantitative details of the measured interaction forces.

The effects of cationic surfactants are observed to be significantly more complicated than those of anionic surfactants, due to the fact that MTAB can actively adsorb to both surfaces and modify their corresponding surface properties accordingly.

3.3. Polycationic Surfactant Monolayers and Multi-component Films. For the sake of simplicity, the polyelectrolyte surfactant bq5x-PDMS was only adsorbed onto the PDMS film, where the PDMS chains of the surfactants can entangle with the PDMS chains that are grafted to the gold

surface. Thus, the mica remained negatively charged, while the PDMS surface adopted a positive charge due to the adsorption of the cationic bq5x-PDMS. The interaction between the mica and the bq5x-PDMS functionalized surface is fully attractive, as shown in Figure 4A. The interaction becomes significantly shorter-ranged when increasing the salt concentration from 1 mM NaCl (blue points and curve, Figure 4A) to 5 mM NaCl (green points and curve, Figure 4A), a signature behavior of electrostatic double layer interactions. The interactions in this case are analyzed with a simple DLVO model that includes contributions from van der Waals and asymmetric electrostatic double layer interactions, as shown in eq 7, where all parameters have been previously described in Section 3.1.

$$W(D) = -\frac{1}{12\pi} \left(\frac{A_{mPg}}{D^2} + \frac{A_{mwP}}{(D - T_H)^2} \right) + \varepsilon \varepsilon_0 \kappa \left[\frac{2\psi_m \psi_p e^{-\kappa(D-T_H)} - (\psi_m^2 + \psi_p^2) e^{-2\kappa(D-T_H)}}{1 - e^{-2\kappa(D-T_H)}} \right] \quad (7)$$

Because ψ_m is measured in a separate experiment, and the Debye length is calculated from eq 2 above, the only fitting parameter in eq 7 is ψ_{bq5x} , the surface potential of the bq5x-PDMS functionalized surface. The data are described quantitatively by eq 7 for both 1 mM NaCl and 5 mM NaCl, indicating that the measured attraction is due to an attractive electrostatic double-layer force between the asymmetric double layers. The fitting reveals that ψ_{bq5x} decreases from 60 mV at 1 mM NaCl to 40 mV at 5 mM NaCl, which is the expected trend for the surface potential as a function of increasing salt concentration. Repeat experiments on completely different experimental set-ups and days resulted in a wide range of ψ_{bq5x} as shown in the Supporting Information. This variance likely comes from variance in the prepared layers, due to slight differences in the adsorption structure and coverage of the bq5x-PDMS layer on the grafted PDMS layer.

The strong measured adhesion energy, $W_{ad} = -10.6 \text{ mJ/m}^2$, is possibly due to specific interactions of the bq5x-PDMS headgroups with mica. Quaternary ammonium groups are known to strongly interact with negatively charged mica surface sites.^{15,22,41} It is unclear if the asymmetric double layer force can be extrapolated to contact or if the adhesion is purely due to this specific amine–mica interaction. Interestingly, these force runs are fully reproducible, i.e., subsequent approach/separation cycles at the same position result in identical data, indicating that no bq5x-PDMS molecules are being pulled out from the layers during the force runs. This is a notable difference from our previous experiments with bq-PDMS surfaces, as discussed below.

Lastly, the effect of adding SDS cosurfactants to the system with adsorbed bq5x-PDMS was examined, as shown in Figure 4B. Addition of SDS results in a monotonic repulsion during both approach and separation of the surfaces. Once again, these forces are analyzed with a DLVO model, eq 7, which indicates that the positive charge on the bq5x-PDMS surface has been reversed and is now strongly negative, resulting in the fitted value of $\psi_{bq5x+SDS} = -100 \text{ mV}$. The SDS appears to have strongly adsorbed into the PDMS layer, reversing the cationic charge of the bq5x-PDMS surface, perhaps removing some bq5x-PDMS, and resulting in an overall strong electrostatic repulsion with the mica.

4. DISCUSSION

Self-assembled surface structures are varied and complex.^{1,18,20–22} At an interface, surfactant equilibrium structure depends on the chemistry and structure of the surface, the chemistry and structure of the surfactant, and the concentration of surfactants in the solution. By measuring the interactions between a hydrophobic polymer surface and a mineral surface in surfactant solutions, we have explored a diverse range of self-assembly phenomena and forces.

At the PDMS–water interface, both anionic and cationic surfactants, polyelectrolytes, and multicomponent mixtures of polyelectrolytes and surfactants adsorb through hydrophobic interactions to form monolayers, or slightly interdigitated monolayers, at the surface. At the mica–water interface, anionic surfactants do not adsorb, while cationic surfactants form monolayers ($C < \text{CMC}$) or fluid bilayers ($C \sim \text{CMC}$). Despite the variety and complexity of self-assembled surface structures, the well-known theories of electrostatic double layers, hydrophobicity, hydration, and van der Waals energies combine to describe the interactions between these self-assembled films in solution. These fundamental potentials quantitatively account for the interactions described in this study, including monotonic repulsions, monotonic attractions, nonmonotonic interactions, bilayer fusion events, and strong adhesion forces due to Coulombic or hydrophobic interactions.

The insights gained through force measurements at the PDMS–surfactant interface translate to physical properties that are relevant for colloidal stability and wetting phenomena. SDS preserves a high surface charge on PDMS, even at increased salt concentrations, and should maintain the stability of silicone emulsions. MTAB reverses the surface charge at the PDMS surface. The concentration of MTAB (above or below the CMC) should result in markedly different flocculation and stability of mineral slurries: below the CMC, monolayers of the cationic surfactant adsorb and hydrophobize the mineral surface, leading to rapid flocculation of a suspension; above the CMC, fluid bilayers on the mineral surface result in metastable suspensions that resist flocculation due to repulsive electrostatic, headgroup hydration, and bilayer stress energies. The concentration of the surfactant in solution also regulates the viscosity and frictional losses near an interface; below the CMC, the exposed hydrophobic MTAB tails may result in a finite hydrodynamic slip plane (reducing friction), while above the CMC, the exposed hydrated surfactant headgroups result in a zero-slip boundary condition and increased interfacial water viscosity.^{42,43}

The silicone-based bq5x-PDMS surfactant is dispersible in water—despite a large hydrophobic polymer domain—and functions as a practical adhesive in the interface between hydrophobic silicone films and negatively charged hydrophilic surfaces. Unlike short-chain aliphatic surfactants, long-chain PDMS surfactants do not rapidly desorb from a hydrophobic PDMS interface—due to increased hydrophobic interactions and interdigitation (entanglements) with the polymer midblock—resulting in a functionalized PDMS surface that maintains adhesive ability in surfactant-depleted solutions. In the interactions with MTAB solutions, bq5x-PDMS, and the previously studied bq-PDMS, the mechanism that supports adhesion between the mica and PDMS surfaces is initially the same: electrostatic interactions bind the surfactant headgroups to the mica surface, while hydrophobic interactions between the surfactant tail (or midblock) maintain the adhesive bridge to

the PDMS surface. Yet interestingly, the adhesive bridge fails along different planes for these surfactants. For MTAB and bq-PDMS, the adhesion breaks along the hydrophobic interface (MTAB tail/PDMS interface, or bq-PDMS midblock/PDMS interface) and corresponds to a large adhesion energy that approaches the expected thermodynamic adhesion between 2 hydrophobic surfaces ($2\gamma_i \sim 80\text{--}100 \text{ mJ/m}^2$). However, in bq5x-PDMS experiments, the adhesion fails at the interface between the bq5x-PDMS quaternary ammonium headgroups and the mica surface, constituting a break in interfacial electrostatic (Coulombic) bonds that result in a lower overall adhesion energy and zero mass transfer of the bq5x-PDMS surfactant onto the mica surface.

Thus, increasing the number of end group cations in silicone surfactants actually reduces their overall adhesion to negatively charged surfaces. This type of “bond saturation” has been previously observed to reduce the adhesive performance in other systems,⁴⁴ and we speculate that it is caused by adverse competition for binding sites between mobile neighboring headgroups, a subtle geometry constraint of the end group structure, or counterion condensation. In applications that require robust adhesion of silicones to negatively charged surfaces, such as the adsorption of lubricating PDMS films to natural polymers, minerals, or fabrics, the “less is more” philosophy of reducing the number of cationic end groups can thus promote a strongly bound and longer film lifetime.

Increasing the end group size and charge from bq-PDMS to bq5x-PDMS radically alters how the molecules self-assemble at a silicone film, and correspondingly, the surface forces at the silicone interface. At the PDMS surface, bq-PDMS self-assembles into dynamically fluctuating nanostructures that extend into solution. The surface forces of the bq-PDMS film are long-ranged (extending over tens of nm), time- and temperature-dependent, principally due to bridging interactions that occur between the extended bq-PDMS structures and other approaching surfaces. A 5-fold increase in the end group charge density results in bq5x-PDMS molecules that adsorb to the silicone film as a monolayer, lacking any obvious dynamic fluctuations in the monolayer structure. The bq5x-PDMS monolayers behave as a smeared-out layer of cations and their attractive interactions on approach to mica (for $D > 1$ Debye length) are described by the asymmetric theory of electrostatic double layers. Although bq-PDMS films exhibit a rate-dependent bridging force during separation from mica, the higher-charged bq5x-PDMS films do not exhibit a rate-dependent adhesion force as the Coulombic bonds between the headgroups and mica break before the surfactant polymer segments are pulled out from underlying PDMS surface.

Although the PDMS polyelectrolytes reverse the surface charge at PDMS and mediate strong adhesion energy to negatively charged surfaces, low concentrations of anionic surfactants can completely eliminate this adhesive functionality. At a concentration of $\sim 1/8$ th CMC, SDS molecules overadsorb to the PDMS–polyelectrolyte interface, resulting in charge-reversal behavior that causes the PDMS–polyelectrolyte–SDS structure to carry an overall negative surface charge. Presumably, conscious control over both the headgroup charge density of the PDMS polyelectrolyte and the anionic surfactant concentration would result in the precise control over the PDMS surface charge, with intermediate surface charges between “maximally negative” and “maximally positive”.

The activity and phase stability of emulsions depend on both inter- and intra-aggregate interactions. Interaggregate surface

interactions, e.g., between an emulsion droplet and a surface or between two emulsion droplets, include electrostatic double layer, hydrophobic, steric, and van der Waals forces as shown above. Intra-aggregate molecular interactions within emulsion droplets are also highly significant, e.g., hydrophobic interactions of a surfactant molecule within the oil droplet, or Coulombic interactions between oppositely charged surfactant species. In practice, the SFA measurements presented here primarily measure the interaggregate interaction energy per unit area. Indeed, accurate values of the surfactant adsorption free energies and adsorption profiles to hydrophobic and hydrophilic surfaces,^{45–47} combined with surface forces studies, would account for both the intra- and interaggregate interactions to fully characterize an emulsion’s phase behavior. Given the hydrophobic backbone of bq5x-PDMS, we hypothesize that the polyelectrolyte adsorbs to oil–water interfaces with an adsorption free energy that is larger (more favorable) than the adsorption of more hydrophilic polyelectrolytes.^{45–47}

5. CONCLUSIONS

Overall, the charge and self-assembled structure of ionic surfactants can be used to control the sign, magnitude, and range of the interaction energy between hydrophobic and hydrophilic surfaces in solution. The adsorption of charged species to surfaces modulates the strength and sign of the long-range electrostatic double-layer interaction between the surfaces, and can produce monotonic attractions or repulsions. However, nonmonotonic interactions—and accordingly, finite energy barriers to adhesion—are also possible by adsorbing surfactants that give rise to total interaction energies between two surfaces that are of opposite sign at small and large separation distances. At smaller separation distances, ionic surfactants can modify repulsions through the steric-hydration energy of polar headgroups or through the unfavorable elastic spreading energy between adjacent surfactants in a bilayer; conversely, attractive and adhesive energies are tuned through hydrophobic interactions between surfactant tails and nonpolar surfaces, or from Coulombic interactions between headgroups and charged surfaces.

In any case, the results show how one can rationally design anionic, cationic, polyelectrolyte, and mixed surfactant systems to predict and control the desired static or kinetic stability of various emulsions, dispersions, lubricating thin films, or polymeric adhesives. The self-assembly of silicone polyelectrolytes offers an additional level of control over the surface forces and energies: by modifying the end group charge density of the polyelectrolyte, we can incorporate dynamic (rate-dependent) behavior into a system via soft nanostructures,²² and we can control the equilibrium adhesion energy of a PDMS–polyelectrolyte–mica junction. Thus, these silicone polyelectrolytes can serve as tunable adhesives to directly deposit thin silicone films at target surfaces for lubrication and controlled wetting applications.

■ ASSOCIATED CONTENT

Supporting Information

Additional force–distance measurements for bq5x-PDMS adsorbed onto PDMS. The Supporting Information is available free of charge on the ACS Publications website at DOI: 10.1021/acs.langmuir.5b01781.

■ AUTHOR INFORMATION

Corresponding Author

*Jacob@engineering.ucsb.edu.

Notes

The authors declare no competing financial interest.

■ ACKNOWLEDGMENTS

This work was supported by a gift from the Procter & Gamble Company. M.V.R acknowledges support from a NSF Graduate Research Fellowship.

■ REFERENCES

- (1) Zhang, R.; Somasundaran, P. Advances in Adsorption of Surfactants and Their Mixtures at Solid/solution Interfaces. *Adv. Colloid Interface Sci.* **2006**, *123–126*, 213–229.
- (2) De Gennes, P. G.; Taupin, C. Microemulsions and the Flexibility of Oil/water Interfaces. *J. Phys. Chem.* **1982**, *86*, 2294–2304.
- (3) Somasundaran, P.; Mehta, S. C.; Purohit, P. Silicone Emulsions. *Adv. Colloid Interface Sci.* **2006**, *128–130*, 103–109.
- (4) Kim, J.; Gao, Y.; Hebebrand, C.; Peirtsegale, E.; Helgeson, M. E. Polymer–surfactant Complexation as a Generic Route to Responsive Viscoelastic Nanoemulsions. *Soft Matter* **2013**, *9*, 6897.
- (5) Hunter, T. N.; Pugh, R. J.; Franks, G. V.; Jameson, G. J. The Role of Particles in Stabilising Foams and Emulsions. *Adv. Colloid Interface Sci.* **2008**, *137*, 57–81.
- (6) Antonietti, M.; Conrad, J.; Thuenemann, A. Polyelectrolyte-Surfactant Complexes: A New Type of Solid, Mesomorphous Material. *Macromolecules* **1994**, *27*, 6007–6011.
- (7) Banerjee, S.; Cazeneuve, C.; Baghdadli, N.; Ringeissen, S.; Leermakers, F. A. M.; Luengo, G. S. Surfactant-Polymer Interactions: Molecular Architecture Does Matter. *Soft Matter* **2015**, *11*, 2504.
- (8) Faul, C. F. J.; Antonietti, M. Ionic Self-Assembly: Facile Synthesis of Supramolecular Materials. *Adv. Mater.* **2003**, *15*, 673–683.
- (9) Gonzenbach, U. T.; Studart, A. R.; Tervoort, E.; Gauckler, L. J. Ultrastable Particle-Stabilized Foams. *Angew. Chem., Int. Ed.* **2006**, *45*, 3526–3530.
- (10) Helgeson, M. E.; Moran, S. E.; An, H. Z.; Doyle, P. S. Mesoporous Organohydrogels from Thermogelling Photocrosslinkable Nanoemulsions. *Nat. Mater.* **2012**, *11*, 344–352.
- (11) Mehta, G.; Kiel, M. J.; Lee, J. W.; Kotov, N.; Linderman, J. J.; Takayama, S. Polyelectrolyte-Clay-Protein Layer Films on Microfluidic PDMS Bioreactor Surfaces for Primary Murine Bone Marrow Culture. *Adv. Funct. Mater.* **2007**, *17*, 2701–2709.
- (12) Murarash, B.; Itovich, Y.; Varenberg, M. Tuning Elastomer Friction by Hexagonal Surface Patterning. *Soft Matter* **2011**, *7*, 5553.
- (13) Noro, A.; Hayashi, M.; Matsushita, Y. Design and Properties of Supramolecular Polymer Gels. *Soft Matter* **2012**, *8*, 6416.
- (14) Israelachvili, J. N. *Intermolecular and Surface Forces*, 3rd ed.; Academic Press: Waltham, MA, 2011.
- (15) Chen, Y. L.; Chen, S.; Frank, C.; Israelachvili, J. Molecular Mechanisms and Kinetics during the Self-Assembly of Surfactant Layers. *J. Colloid Interface Sci.* **1992**, *153*, 244–265.
- (16) Ducker, W. A.; Grant, L. M. Effect of Substrate Hydrophobicity on Surfactant Surface–Aggregate Geometry. *J. Phys. Chem.* **1996**, *100*, 11507–11511.
- (17) Wanless, E. J.; Ducker, W. A. Organization of Sodium Dodecyl Sulfate at the Graphite–Solution Interface. *J. Phys. Chem.* **1996**, *100*, 3207–3214.
- (18) Ducker, W. A.; Wanless, E. J. Surface-Aggregate Shape Transformation. *Langmuir* **1996**, *12*, 5915–5920.
- (19) Grant, L. M.; Tibergh, F.; Ducker, W. A. Nanometer-Scale Organization of Ethylene Oxide Surfactants on Graphite, Hydrophilic Silica, and Hydrophobic Silica. *J. Phys. Chem. B* **1998**, *102*, 4288–4294.
- (20) Manne, S.; Cleveland, J. P.; Gaub, H. E.; Stucky, G. D.; Hansma, P. K. Direct Visualization of Surfactant Hemimicelles by Force Microscopy of the Electrical Double Layer. *Langmuir* **1994**, *10*, 4409–4413.
- (21) Manne, S.; Gaub, H. E. Molecular Organization of Surfactants at Solid-Liquid Interfaces. *Science (Washington, DC, U. S.)* **1995**, *270*, 1480–1482.
- (22) Rapp, M. V.; Donaldson, S. H.; Gebbie, M. A.; Das, S.; Kaufman, Y.; Gizaw, Y.; Koenig, P.; Roiter, Y.; Israelachvili, J. N. Hydrophobic, Electrostatic, and Dynamic Polymer Forces at Silicone Surfaces Modified with Long-Chain Bolaform Surfactants. *Small* **2015**, *11*, 2058.
- (23) Israelachvili, J.; Min, Y.; Akbulut, M.; Alig, A.; Carver, G.; Greene, W.; Kristiansen, K.; Meyer, E.; Pesika, N.; Rosenberg, K.; et al. Recent Advances in the Surface Forces Apparatus (SFA) Technique. *Rep. Prog. Phys.* **2010**, *73*, 036601.
- (24) Johnson, K. L.; Kendall, K.; Roberts, A. D. Surface Energy and the Contact of Elastic Solids. *Proc. R. Soc. London, Ser. A* **1971**, *324*, 301–313.
- (25) Donaldson, S. H.; Das, S.; Gebbie, M. A.; Rapp, M.; Jones, L. C.; Roiter, Y.; Koenig, P. H.; Gizaw, Y.; Israelachvili, J. N. Asymmetric Electrostatic and Hydrophobic-Hydrophilic Interaction Forces between Mica Surfaces and Silicone Polymer Thin Films. *ACS Nano* **2013**, *7*, 10094–10104.
- (26) Hegner, M.; Wagner, P.; Semenza, G. Ultralarge Atomically Flat Template-Stripped Au Surfaces for Scanning Probe Microscopy. *Surf. Sci.* **1993**, *291*, 39–46.
- (27) Chai, L.; Klein, J. Large Area, Molecularly Smooth (0.2 Nm Rms) Gold Films for Surface Forces and Other Studies. *Langmuir* **2007**, *23*, 7777–7783.
- (28) Donaldson, S. H.; Røyne, A.; Kristiansen, K.; Rapp, M. V.; Das, S.; Gebbie, M. A.; Lee, D. W.; Stock, P.; Valtiner, M.; Israelachvili, J. Developing a General Interaction Potential for Hydrophobic and Hydrophilic Interactions. *Langmuir* **2015**, *31*, 2051–2064.
- (29) Tian, C. S.; Shen, Y. R. Structure and Charging of Hydrophobic Material/water Interfaces Studied by Phase-Sensitive Sum-Frequency Vibrational Spectroscopy. *Proc. Natl. Acad. Sci. U. S. A.* **2009**, *106*, 15148–15153.
- (30) Creux, P.; Lachaise, J.; Gracia, A.; Beattie, J. K.; Djerdjev, A. M. Strong Specific Hydroxide Ion Binding at the Pristine Oil/water and Air/water Interfaces. *J. Phys. Chem. B* **2009**, *113*, 14146–14150.
- (31) Hogg, R.; Healy, T. W.; Fuerstenau, D. W. Mutual Coagulation of Colloidal Dispersions. *Trans. Faraday Soc.* **1966**, *62*, 1638.
- (32) Parsegian, V. A.; Gingell, D. On the Electrostatic Interaction across a Salt Solution between Two Bodies Bearing Unequal Charges. *Biophys. J.* **1972**, *12*, 1192–1204.
- (33) Donaldson, S. H.; Lee, C. T.; Chmelka, B. F.; Israelachvili, J. N. General Hydrophobic Interaction Potential for Surfactant/lipid Bilayers from Direct Force Measurements between Light-Modulated Bilayers. *Proc. Natl. Acad. Sci. U. S. A.* **2011**, *108*, 15699–15704.
- (34) Mittal, K. L.; Bothorel, P., Eds. *Surfactants in Solution*; Springer US: Boston, MA, 1987.
- (35) Israelachvili, J.; Pashley, R. The Hydrophobic Interaction Is Long Range, Decaying Exponentially with Distance. *Nature* **1982**, *300*, 341–342.
- (36) Subramanian, V.; Ducker, W. Proximal Adsorption of Cationic Surfactant on Silica at Equilibrium. *J. Phys. Chem. B* **2001**, *105*, 1389–1402.
- (37) Lokar, W. J.; Ducker, W. A. Proximal Adsorption at Glass Surfaces: Ionic Strength, pH, Chain Length Effects. *Langmuir* **2004**, *20*, 378–388.
- (38) Evans, E.; Metcalfe, M. Free Energy Potential for Aggregation of Giant, Neutral Lipid Bilayer Vesicles by Van Der Waals Attraction. *Biophys. J.* **1984**, *46*, 423–426.
- (39) Servuss, R. M.; Helfrich, W. Mutual Adhesion of Lecithin Membranes at Ultralow Tensions. *J. Phys. (Paris)* **1989**, *50*, 809–827.
- (40) Banquy, X.; Kristiansen, K.; Lee, D. W.; Israelachvili, J. N. Adhesion and Hemifusion of Cytoplasmic Myelin Lipid Membranes Are Highly Dependent on the Lipid Composition. *Biochim. Biophys. Acta, Biomembr.* **2012**, *1818*, 402–410.
- (41) Claesson, P.; Horn, R. G.; Pashley, R. M. Measurement of Surface Forces between Mica Sheets Immersed in Aqueous

Quaternary Ammonium Ion Solutions. *J. Colloid Interface Sci.* **1984**, *100*, 250–263.

(42) Audry, M.-C.; Piednoir, A.; Joseph, P.; Charlaix, E. Amplification of Electro-Osmotic Flows by Wall Slippage: Direct Measurements on OTS-Surfaces. *Faraday Discuss.* **2010**, *146*, 113.

(43) Honig, C. D. F.; Ducker, W. A. Squeeze Film Lubrication in Silicone Oil: Experimental Test of the No-Slip Boundary Condition at Solid–Liquid Interfaces. *J. Phys. Chem. C* **2008**, *112*, 17324–17330.

(44) Wang, J.; Tahir, M. N.; Kappl, M.; Tremel, W.; Metz, N.; Barz, M.; Theato, P.; Butt, H.-J. Influence of Binding-Site Density in Wet Bioadhesion. *Adv. Mater.* **2008**, *20*, 3872–3876.

(45) Li, D.; Schubert, B.; Wagner, N. J. Characterization of Cationic Polyelectrolytes Adsorption to an Anionic Emulsion via Zeta-Potential and Microcalorimetry. *J. Surfactants Deterg.* **2014**, *17*, 655–667.

(46) Li, D.; Kelkar, M. S.; Wagner, N. J. Phase Behavior and Molecular Thermodynamics of Coacervation in Oppositely Charged Polyelectrolyte/surfactant Systems: A Cationic Polymer JR 400 and Anionic Surfactant SDS Mixture. *Langmuir* **2012**, *28*, 10348–10362.

(47) Seng, W. P.; Tam, K. C.; Jenkins, R. D.; Bassett, D. R. Calorimetric Studies of Model Hydrophobically Modified Alkali-Soluble Emulsion Polymers with Varying Spacer Chain Length in Ionic Surfactant Solutions. *Macromolecules* **2000**, *33*, 1727–1733.